Exploring (NH2F)2, H2FP:NFH2, and (PH2F)2 potential surfaces: hydrogen bonds or pnicogen bonds?

ARTICLE *in* THE JOURNAL OF PHYSICAL CHEMISTRY A · DECEMBER 2012

Impact Factor: 2.69 · DOI: 10.1021/jp3100816 · Source: PubMed

4 AUTHORS, INCLUDING:

Ibon Alkorta
Spanish National Research Council
680 PUBLICATIONS **12,430** CITATIONS
SEE PROFILE

Goar Sánchez
University College Dublin
69 PUBLICATIONS **905** CITATIONS
SEE PROFILE

José Elguero
Spanish National Research Council
1,502 PUBLICATIONS **22,206** CITATIONS
SEE PROFILE

THE JOURNAL OF PHYSICAL CHEMISTRY A

Article

pubs.acs.org/JPCA

Exploring $(NH_2F)_2$, $H_2FP{:}NFH_2$, and $(PH_2F)_2$ Potential Surfaces: Hydrogen Bonds or Pnicogen Bonds?

Ibon Alkorta,*[,†] Goar Sánchez-Sanz,[†] José Elguero,[†] and Janet E. Del Bene*[,‡]

[†]Instituto de Química Médica (C.S.I.C.), Juan de la Cierva 3, E-28006 Madrid, Spain

[‡]Department of Chemistry, Youngstown State University, Youngstown, Ohio 44555, United States

Supporting Information

ABSTRACT: An ab initio MP2/aug'-cc-pVTZ study has been carried out to identify local minima on the $(NH_2F)_2$, $H_2FP{:}NFH_2$, and $(PH_2F)_2$ potential surfaces, to characterize the types of interactions which stabilize the complexes found at these minima, and to evaluate their binding energies. With one exception, $(NH_2F)_2$ complexes are stabilized by N−H···N or N−H···F hydrogen bonds. Only one complex, that with the smallest binding energy, has a pnicogen N···N bond. In contrast, $(PH_2F)_2$ complexes are stabilized by P···P or P···F pnicogen bonds or by an antiparallel alignment of the dipole moment vectors of the two monomers, but not by hydrogen bonds. The most stable complex has an F−P···P−F alignment which approaches linearity. Both hydrogen-bonded and pnicogen-bonded complexes exist on the $H_2FP{:}NFH_2$ surface, with the most stable being the pnicogen-bonded complex with F−P···N−F approaching a linear arrangement. Charge transfer transitions from a lone pair on a P, N, or F atom in one molecule to an antibonding σ^* orbital of the other stabilize these complexes. These transitions are most important for complexes with pnicogen bonds. Although net charge transfer occurs in complexes in which the two monomers are inequivalent, charges on N and P do not correlate with N and P absolute chemical shieldings. Rather, these shieldings also reflect charge distributions and overall bonding patterns. EOM-CCSD two-bond spin−spin coupling constants $^{2h}J(X{-}Y)$ across X−H···Y hydrogen bonds tend to be small, due in part to the nonlinearity of many of the hydrogen bonds. ^{1p}J values across a particular kind of pnicogen bond are relatively large and vary significantly but do not correlate with corresponding distances.

INTRODUCTION

Supramolecular structures, which are well-defined and permanent in the solid state,[1,2] are mobile, dynamic, and adaptive in solution.[3] Both, however, depend upon the strengths, geometries, and directionality of intermolecular interactions. There are many types of intermolecular interactions, perhaps the most well-known of which are hydrogen bonds, denoted as X−H···Y,[4−6] and halogen bonds, X−Cl···Y.[7−9] In both of these, X−H and X−Cl are the Lewis acids, and the Lewis base is the molecule containing atom Y. The newest member of the family of intermolecular interactions is the pnicogen bond. Although still in its infancy, the pnicogen bond has received considerable attention in the recent literature.[10−30] This bond is defined as an inter- or possibly an intramolecular interaction in which an atom from group 15 acts as a Lewis acid, that is, as an electron-pair acceptor. The simplest complexes stabilized by pnicogen bonds are $(PH_3)_2$ and $H_3P{:}NH_3$. Their potential surfaces exhibit two minima, one pnicogen-bonded and the other hydrogen-bonded, with the pnicogen-bonded complex being the global minimum.[12] The related ammonia dimer $(NH_3)_2$ is known both experimentally and theoretically to adopt a C_s fluxional minimum with a low-barrier transition state of C_{2h} symmetry, which interchanges the roles of the hydrogen-bond donor and acceptor molecules.[31] However, no stable complex with an N···N pnicogen bond has been found on the potential surface.

We have recently investigated P···P and P···N pnicogen bonds in complexes $(PH_2X)_2$,[22] $H_2XP{:}NXH_2$,[23] and $(PHFX)_2$,[27] with a variety of substituents X. Of these, the most stable complexes have an F−P···P−F arrangement that approaches linearity. However, on the $(NH_2F)_2$, $H_2FP{:}NFH_2$, and $(PH_2F)_2$ surfaces, there are undoubtedly other stable complexes which have yet to be investigated. In the present study, we ask what types of minima exist on these surfaces, what are the structures of the equilibrium complexes found at these minima, and how do they compare energetically. To further characterize equilibrium complexes, we have analyzed the nature of their intermolecular bonds and electron distributions, and their NMR properties of ^{15}N and ^{31}P chemical shieldings and indirect spin−spin coupling constants across intermolecular bonds. In this article we report the results of our study.

COMPUTATIONAL METHODS

The structures of isolated monomers and complexes were optimized at second-order Møller−Plesset perturbation theory (MP2)[32−35] with the aug'-cc-pVTZ basis set,[36] which is the Dunning aug-cc-pVTZ basis set[37,38] with diffuse functions removed from H atoms. Frequencies were computed to identify local minima and transition structures on the surfaces.

Received: October 11, 2012
Published: December 20, 2012

Optimization and frequency calculations were performed using the Gaussian09 program.[39]

Electron densities of complexes have been analyzed employing the Atoms in Molecules (AIM) methodology[40,41] with the AIMAll program.[42] The Natural Bond Orbital (NBO) method[43] has been used to obtain atomic charges and analyze charge-transfer interactions between occupied and virtual orbitals using the NBO-5 program[44] within the Gamess program.[45] The molecular electrostatic potential (MEP) has been calculated and represented on the 0.001 au electron density isosurface using the WFA program.[46] This isosurface has been shown to resemble the van der Waals surface.[47]

MP2/aug'-cc-pVTZ absolute chemical shieldings have been calculated within the GIAO approximation.[48] Coupling constants were evaluated using the equation-of-motion coupled cluster singles and doubles (EOM-CCSD) method in the CI (configuration interaction)-like approximation,[49,50] with all electrons correlated. For these calculations, the Ahlrichs[51] qzp basis set was placed on ^{19}F and ^{15}N, and the qz2p basis set on ^{31}P and ^{1}H. The EOM-CCSD calculations were performed using ACES II[52] on the IBM Cluster 1350 (Glenn) at the Ohio Supercomputer Center.

RESULTS AND DISCUSSION

This section has been divided into four subsections. Characteristics of the monomers NH_2F and PH_2F are described in the first section. The second provides the naming conventions used to identify and distinguish local minima on each surface, and discusses the structures and binding energies of complexes which are found there. In section three, the electronic properties of these complexes are analyzed using the NBO and AIM methodologies. The fourth section is devoted to the NMR properties of chemical shieldings and spin−spin coupling constants.

Molecular Properties of the Isolated Monomers. The geometry, dipole moment, and inversion barrier of the NH_2F molecule have been obtained from microwave spectroscopy.[53] The millimeter-wavelength and infrared spectra have been used to derive the ground state geometry of PH_2F.[54] The experimental results and corresponding computed MP2-aug'-cc-pVTZ data are in very good agreement, as evident from Table 1.

The electronic property of the two monomers which is of most interest in this study, is the molecular electrostatic potential (MEP) on the 0.001 au electron density isosurface. The MEP is useful as a tool for identifying basic and acidic sites for possible intermolecular interactions. Negative regions of the MEP are associated with electrophilic sites, while positive MEPs are indicative of nucleophilic sites.

The MEP on the 0.001 au electron density isosurface of the NH_2F molecule is depicted in Figure 1. It indicates that there are two negative regions, one associated with the nitrogen atom with a minimum value of −0.046 au, and the other with the fluorine atom with a minimum value of −0.038 au. The most positive values on the surface are near the two hydrogen atoms with values of 0.063 au, while the σ-hole at N has a value of 0.052 au. In contrast, Figure 1 shows that the most negative MEP for the PH_2F molecule is at the F atom with a value of −0.028 au, while the negative region associated with the lone pair on P has a value of −0.019 au. The most positive region on the electron density isosurface belongs to the σ-hole at P with a value of 0.061 au, while the positive regions at the H atoms have values of 0.030 au. From the MEPs alone, it should be expected that the $(NH_2F)_2$ and $(PH_2F)_2$ potential surfaces should be dramatically different.

Table 1. Computed and Experimental Bond Distances (Å), Bond Angles (deg), Dipole Moments (Debye), and Inversion Barriers (kJ/mol) of NH_2F and PH_2F

parameter	NH_2F calcd	NH_2F exptl	PH_2F calcd	PH_2F exptl
R(N−F)/R(P−F)	1.423	1.4329	1.622	1.602
R(N−H)/R(P−H)	1.018	1.0225	1.416	1.415
∠F−N−H/∠F−P−H	101.5	101.08	97.8	97.8
∠H−N−H/∠H−P−H	105.2	106.27	92.3	92.0
dipole moment[a]	2.28	2.27	1.45	
inversion barrier	64.0	62.2	213.6	

[a]For NH_3, the negative end of the dipole moment vector is at N; for PH_3, the positive end is at P.

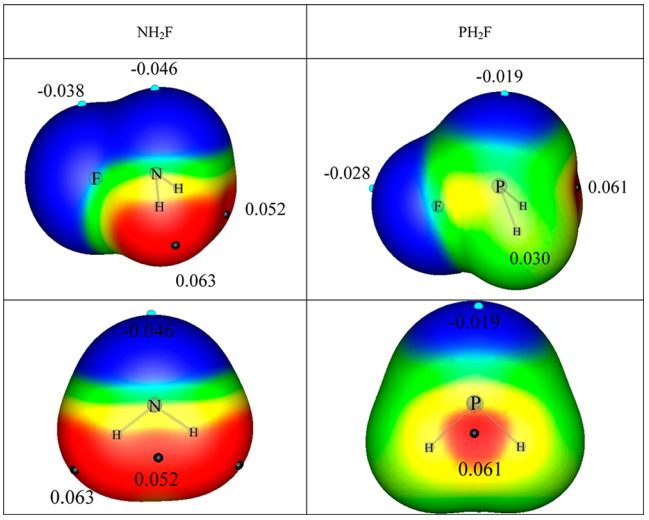

Figure 1. Molecular electrostatic potential on the 0.001 au electron density isosurfaces of NH_2F and PH_2F. Color code: red > 0.04 > yellow > 0.02 > green > 0.00 > blue. The positions of the local minima and maxima on the isosurface are indicated with light blue and black dots, respectively.

Structures and Binding Energies of Complexes. A total of 5, 6, and 8 unique local minima have been located on the potential energy surfaces of $(NH_2F)_2$, $H_2FN{:}PFH_2$, and $(PH_2F)_2$, respectively. These complexes are illustrated in Figures 2−4. The energies and structures of these complexes are also reported in Tables S1 and S2, respectively, of the Supporting Information. The binding energy of each complex is defined as the negative energy for the reaction which forms the complex from the corresponding isolated monomers.

$$\Delta E = -[E(\text{complex}) - \sum_i E_i(\text{monomers})] \quad (1)$$

In order to distinguish the various isomers on a particular potential surface, the following naming convention has been employed. If the isomer is stabilized by only a pnicogen bond, the name is pnicab, where a and b are the atoms that form the pnicogen bond. If another complex is stabilized by a pnicogen bond involving the same a and b, the designations are pnicab-1 and pnicab-2, with the former more stable than the latter. Complexes stabilized by hydrogen bonds are designated hbxhy,

dx.doi.org/10.1021/jp3100816 | J. Phys. Chem. A 2013, 117, 183−191

with X and Y the atoms that form the X−H···Y hydrogen bond. If there are two hydrogen bonds in the complex, the designation is hb2xhy. If both pnicogen and hydrogen bonds are present, the complex is designated pnicabhbxhy.

On the $(PH_2F)_2$ surface there are three complexes with P···P pnicogen bonds, designated as pnicpp-fppf, pnicpp-fpph, and pnicpp-hpph, with the second field indicating the atoms that approach a nearly linear P···P−F or P···P−H arrangement. There are also three equilibrium $(PH_2F)_2$ isomers stabilized by P···F pnicogen bonds, designated as pnicpf-tg, pnicpf-tc, and pnicpf-cc. The second field describes two structural parameters that distinguish these isomers. The first is the relative orientation with respect to the intermolecular P···F bond, of the P−F bond of the molecule containing the lone pair electron-donor atom F (the base), and the PH_2 group of the molecule containing the electron-acceptor atom P (the acid). There are only two orientations, cis (c) and trans (t). The second is the relative orientation of the two PH_2 groups with respect to the P−F bond of the base: cis (c), gauche (g), and trans (t). The three equilibrium structures, pnicpf-tg, pnicpf-tc, and pnicpf-cc, are illustrated in Figure 4. Note that pnicpf-tc and pnicpf-cc are related by a 180° rotation of the base around the intermolecular P···F bond. Although three other isomers of this type are possible, they either optimize to another structure or have one imaginary frequency. The final two equilibrium $(PH_2F)_2$ complexes are pdipC2 and pdipCi. These isomers are stabilized by an antiparallel arrangement of monomer dipole moment vectors, with C_2 and C_i symmetries, respectively.

$(NH_2F)_2$. Five unique minima have been located on the $(NH_2F)_2$ potential surface, and these are shown in Figure 2. The two most stable structures are hbnhn-1 and hbnhn-2, with binding energies of 21.6 and 20.9 kJ/mol, respectively. hbnhn-1 has a relatively short N−N distance and is stabilized by a nonlinear N−H···N hydrogen bond. hbnhn-2 has a longer N−N distance and is stabilized by a nonlinear N−H···N hydrogen bond and secondarily by a long-range electrostatic H···F interaction. The next two dimers in order of decreasing stability are hb2nhfC1 and hb2nhfC2, with binding energies of 20.0 and 19.3 kJ/mol, respectively. These two dimers are structurally and energetically similar, being stabilized by two distorted N−H···F hydrogen bonds, which are nonequivalent in the C_1 structure but equivalent in the C_2. There are two degenerate hb2nhfC1 structures on the potential surface, which are separated by a transition state of C_i symmetry, with a barrier of only 0.2 kJ/mol. In contrast, the conversion of hb2nhfC1 into hb2nhfC2 requires the inversion of one of the NH_2F molecules, with the transition state providing a barrier of 64.3 kJ/mol. Since the barrier is greater than the binding energies of these complexes, the more favorable path to convert hb2nhfC1 into hb2nhfC2 would proceed via dissociation and then reassociation of the two monomers.

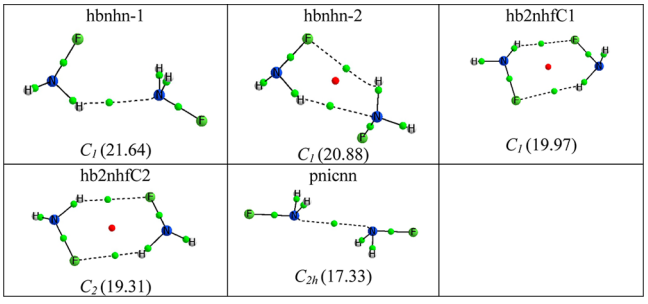

Figure 2. Molecular graphs for optimized geometries, symmetries, and binding energies (kJ/mol) of dimers $(NH_2F)_2$. Green and red dots indicate the positions of bond and ring critical points, respectively.

On the $(NH_2F)_2$ surface, there is only one complex stabilized by a pnicogen bond, and that is pnicnn. Complex pnicnn has an N···N pnicogen bond and is the least stable complex on the surface with a binding energy of 17.3 kJ/mol. Although the potential surface was searched for a complex with an N···F pnicogen bond, no stable complex was found. The absence of such a complex most probably reflects the combination of the relatively poor electron-pair donor atom (F) with the relatively poor electron-pair acceptor atom (N). Thus, hydrogen bonding is by far the preferred mode of intermolecular interaction on the $(NH_2F)_2$ potential surface.

$H_2FP:NFH_2$. Equilibrium structures of complexes $H_2FP:NFH_2$ are shown in Figure 3. The global minimum on the $H_2FP:NFH_2$ surface corresponds to the complex pnicpn. This complex has a P···N pnicogen bond with a F−P···N−F alignment which approaches linearity, and a binding energy of 26.7 kJ/mol. Next in stability is the complex pnicpf-1, which is stabilized by a P···F pnicogen bond and a secondary long-range P···H interaction, resulting in a binding energy of 17.1 kJ/mol. The remaining four complexes on the surface have binding energies between 14.7 and 13.4 kJ/mol. Two of these, pnicpfhbnhf-1 and pnicpfhbnhf-2 with C_1 symmetry, are stabilized by both P···F pnicogen bonds and nonlinear N−H···F hydrogen bonds. Their interconversion requires the inversion of either NH_2F or PH_2F. However, the inversion barriers for these two molecules in the complexes are high at 64.3 and 213.8 kJ/mol, respectively. The remaining complexes, pnicnf and pnicpf-2, are stabilized by N···F and P···F pnicogen bonds, respectively. Thus, unlike the $(NH_2F)_2$ surface, complexes on the $H_2FP:NFH_2$ surface are stabilized either by pnicogen bonds or by a combination of pnicogen and hydrogen bonds.

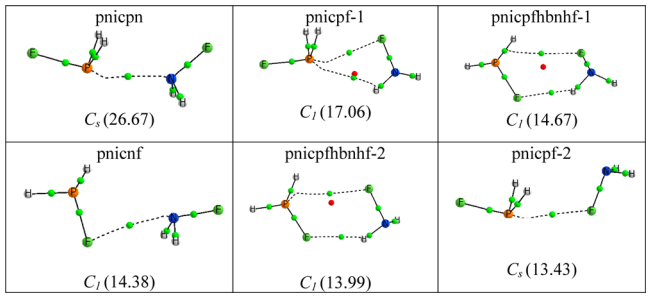

Figure 3. Molecular graphs for optimized geometries, symmetries, and interaction energies (kJ/mol) of $H_2FP:NFH_2$ complexes. Green and red dots indicate the positions of bond and ring critical points, respectively.

$(PH_2F)_2$. In contrast to both the $(NH_2F)_2$ and $H_2FP:NFH_2$ surfaces, the $(PH_2F)_2$ surface has no complexes stabilized by hydrogen bonds. Because of its relatively low electronegativity and the electron-withdrawing effect of F, P bears a high positive charge in PH_2F, and is therefore not a competitive basic site for hydrogen-bond formation. Rather, three $(PH_2F)_2$ complexes are stabilized by P···P pnicogen bonds, three by P···F pnicogen bonds, and two by molecular dipole−dipole interactions, as depicted in Figure 4. The two most stable complexes, pnicpp-fppf and pnicpp-fpph, have binding energies of 34.0 and 18.6

dx.doi.org/10.1021/jp3100816 | J. Phys. Chem. A 2013, 117, 183−191

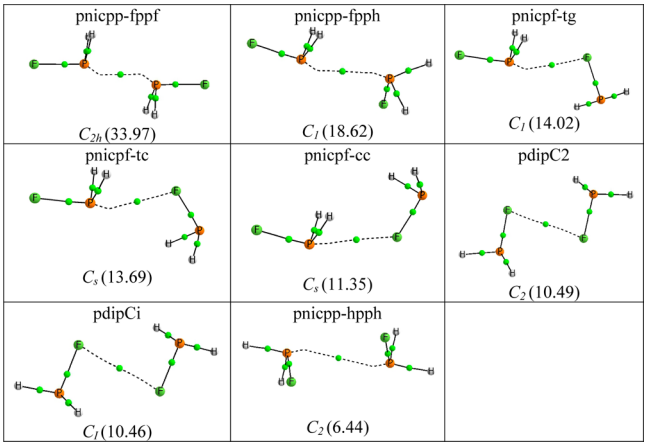

Figure 4. Molecular graphs for optimized geometries, symmetries, and interaction energies (kJ/mol) of $(PH_2F)_2$ dimers. Green dots indicate the positions of bond critical points.

kJ/mol, respectively. The more stable of these has an F−P···P−F alignment, which approaches linearity, while the less stable complex has an F−P···P−H linear arrangement. Complex pnicpp-hpph is the least stable complex on the surface, with a linear H−P···P−H alignment and a binding energy of only 6.4 kJ/mol. These data are consistent with previous studies which demonstrated that linear F−P···P−F and F−P···N−F alignments increase the stabilities of complexes with P···P and P···N pnicogen bonds.[22,23,27]

There are three complexes that are stabilized by P···F pnicogen bonds. These are pnicpf-tg, pnicpf-tc, and pnicpf-cc, with binding energies of 14.0, 13.7, and 11.4 kJ/mol, respectively. For complexes pnicpf-tg and pnicpf-tc, the P−F bond of the base is trans to the PH_2 group of the acid with respect to the intermolecular P···F bond. These two isomers are differentiated by the relative orientation of the PH_2 groups in the two complexes, which are gauche and cis, respectively, with respect to the intramolecular P−F bond of the base. The third isomer, pnicpf-cc, has the intramolecular P−F bond of the base cis to the PH_2 group of the acid, and the PH_2 groups of the two molecules cis to each other with respect to the P−F bond of the base. Complex pnicpf-cc is related to pnicpf-tc by a 180° rotation of the base about the intermolecular P···P bond.

The final two complexes, pdipC2 and pdipCi, are stabilized by an antiparallel alignment of monomer dipole moment vectors, and are differentiated by the relative orientations of the two PH_2 groups. However, both have binding energies of 10.5 kJ/mol. It is most interesting that these two complexes are preferred to hydrogen-bonded complexes on the $(PH_2F)_2$ potential surface.

AIM and NBO Analyses. Topological analyses of the electron densities of these complexes yield a large number of intermolecular bond critical points (BCPs), as evident from Figures 2−4. Bond critical points are found for all of the pnicogen bonds: P···P, P···F, P···N, N···F, and N···N, as well as for N−H···N and N−H···F hydrogen bonds. There are some bond critical points that suggest the presence of a hydrogen bond, but we have not identified the complex as being stabilized by a hydrogen bond. An example is the H_2FP:NFH_2 complex pnicpf-1, for which there is a bond critical point along the path connecting P and H. However, because the N−H···P arrangement deviates significantly from linearity, this interaction has been classified not as a hydrogen bond, but as a secondary long-range electrostatic attraction. In addition, F···F BCPs are found in the two weakly bound $(PH_2F)_2$ complexes pdipC2 and pdipCi, although the interaction between the two F atoms does not stabilize these complexes.

The AIM analyses show that the electron densities at BCPs are less than 0.1 au, the Laplacians of the electron densities are

Table 2. Second-Order Energies (kJ/mol) for Intermolecular Charge Transfer Interactions and Net Charge Transfer (e) for Complexes $(NH_2F)_2$, H_2FP:NFH_2, and $(PH_2F)_2$[a]

complex	charge transfer from	energy	charge transfer from	energy	net charge transfer
$(NH_2F)_2$					
hbnhn-1	lp N(R) → σ*N−H(L)	12.4			0.006
hbnhn-2	lp N(R) → σ*N−H(L)	11.4			0.005
hb2nhfC1	lp F(R) → σ*N−H(L)	7.6	lp F(L) → σ*N−H(R)	5.2	0.001
hb2nhfC2	lp F(R) → σ*N−H(L)	8.7	lp F(L) → σ*N−H(R)	8.7	0.000
pnicnn	lp N(R) → σ*N−F(L)	6.8	lp N(L) → σN−F(R)	6.8	0.000
$(H_2FP:NFH_2)$					
pnicpn	lp N → σ*P−F	53.9	lp P → σ*N−F	12.1	0.047
pnicpf-1	lp F → σ*P−F	14.1	lp P → σ*N−H	3.9	0.008
pnicpfhbnhf-1	lp F → σ*N−H	4.7	lp F → σ*P−H	2.4	0.002
pnicnf	lp N → σ*P−H	4.2	lp F → σ*N−F	4.1	0.005
pnicpfhbnhf-2	lp F → σ*N−H	4.0	lp F → σ*P−H	2.3	0.002
pnicpf-2	lp F → σ*P−F	11.0			0.013
$(PH_2F)_2$					
pnicpp-fppf	lp P(R) → σ*P−F(L)	124.9	lp P(L) → σ*P−F(R)	124.9	0.000
pnicpp-fpph	lp P(R) → σ*P−F(L)	48.4	lp P(L) → σ*P−H(R)	13.1	0.068
pnicpf-tg	lp F(R) → σ*P−F(L)	8.5			0.003
pnicpf-tc	lp F(R) → σ*P−F(L)	9.0			0.009
pnicpf-cc	lp F(R) → σ*P−F(L)	5.5			0.010
pdipC2	none above the threshold				0.000
pdipCi	none above the threshold				0.000
pnicpp-hpph	lp P(R) → σ*P−H(L)	4.7	lp P(L) → σ*P−H(R)	4.7	0.000

[a](L) and (R) refer to the molecules on the left- and right-hand sides of the panels in Figures 2−4.

dx.doi.org/10.1021/jp3100816 | J. Phys. Chem. A 2013, 117, 183−191

positive, and the total energy densities are positive with three exceptions. These data indicate that the bonds in these complexes have little covalent character. Positive energy densities are found for the three complexes with the strongest pnicogen bonds, two complexes on the $(PH_2F)_2$ surface (pnicpp-fppf and pnicpp-fpph), and pnicpn on the $H_2FP{:}NFH_2$ surface. This suggests that the pnicogen bonds in these three complexes have some covalent character.

The second order perturbation energies for the stabilizing intermolecular charge transfer transitions are reported in Table 2. In this table, molecules are distinguished as (L) and (R), where (L) refers to the molecule on the left-hand side of each panel in Figures 2−4, and (R) refers to the molecule on the right. Since in some complexes the same molecule acts as both an acid and a base, it is not appropriate to characterize them simply as acids or bases. However, the panels have been drawn so that in those complexes in which the two molecules are inequivalent, net charge transfer occurs from the molecule on the right to the molecule on the left. Thus, in terms of net charge transfer, the molecule on the right is the base, and that on the left is the acid.

Among the $(NH_2F)_2$ complexes, the two most stabilizing charge-transfer transitions at 12.4 and 11.4 kJ/mol are found for the most stable dimers, hbnhn-1 and hbnhn-2, respectively. Charge transfer occurs from the N lone pair of the proton-acceptor N to the proton donor σ^*N−H orbital. When two hydrogen bonds are present as in hb2nhfC1 and hb2nhfC2, charge transfer interactions occur across both hydrogen bonds, from F to the N−H proton donor. The charge transfer interaction energy is only 6.8 kJ/mol in the most weakly bound complex pnicnn with its N···N pnicogen bond. Net charge transfer is only 0.006e and 0.005e in hbnhn-1 and hbnhn-2, respectively. In the remaining complexes, there is essentially no net charge transfer.

Among the $H_2FP{:}NFH_2$ complexes, the most stabilizing charge transfer interaction is found for the P···N pnicogen bond in the complex pnicpn, for which the lp N → σ^*P−F interaction energy is 53.9 kJ/mol, significantly greater than any charge transfer energy in $(NH_2F)_2$ complexes. In the same complex, the lp P → σ^*N−F transition is significantly less stabilizing at 12.1 kJ/mol. Net charge transfer is significant at 0.05e and occurs from NH_2F to PH_2F, as expected. The lp F→ σ^*P−F energies for the pnicogen-bonded complexes pnicpf-1 and pnicpf-2 are 14.1 and 11.0 kJ/mol, and the net charge transfer from NH_2F to PH_2F is 0.008e and 0.013e, respectively. The charge transfer interaction energies and the net charge transfer for the remaining $H_2FP{:}NFH_2$ complexes are significantly reduced. It is interesting to note that for the pnicnf complex, there is a BCP indicating a N···F pnicogen bond at a distance of 2.720 Å, for which the lp F → σ^*N−F charge transfer energy is 4.1 kJ/mol. Although there is no BCP, there is a lp N → σ^*P−H long-range interaction with a slightly greater charge transfer energy of 4.2 kJ/mol. In this complex, the net charge transfer is from NH_2F to PH_2F, as expected.

The $(PH_2F)_2$ complex pnicpp-fppf is the most stable complex among those investigated in this study, and it also has the largest charge transfer energy of 124.9 kJ/mol for the lp P → σ^*P−F transition. However, since both PH_2F molecules are equivalent, there is no net charge transfer in this complex. The second most stable complex pnicpp-fpph has a lp P(R) → σ^*P−F(L) charge transfer energy of 48.4 kJ/mol. The charge transfer energy for the lp P(L) → σ^*P−H(R) transition is significantly less at 13.1 kJ/mol, again reflecting the decreased stability of a linear H−P···P arrangement. The net charge transfer of 0.068e is to the molecule with P···P−F linear. The smallest charge transfer interaction energy is 4.7 kJ/mol for the least stable complex pnicpp-hpph, which has H−P···P−H linear.

Complexes pnicpf-tg, pnicpf-tc, and pnicpf-cc have significantly reduced charge transfer energies of 8.5, 9.0, and 5.5 kJ/mol, respectively, with a net charge transfer of 0.01e or less. It is interesting to note that the order of charge transfer energies is not the same as the order of binding energies since pnicpf-tg has the greatest binding energy in this group, but charge transfer is greatest for pnicpf-cc. Charge transfer energies for pdipC2 and pdipCi are below the threshold value of 4 kJ/mol.

NMR Properties. *Chemical Shieldings.* The charges on P and N and their absolute chemical shieldings in complexes $(NH_2F)_2$, $H_2FP{:}NFH_2$, and $(PH_2F)_2$ are reported in Table 3.

Table 3. NBO Charges (e) and Absolute Chemical Shieldings (σ, ppm) on P and N in Complexes $(NH_2F)_2$, $H_2FP{:}NFH_2$, and $(PH_2F)_2$[a]

complex	e (L)[b]	σ (L)[b]	e (R)[b]	σ (R)[b]
hbnhn-1	−0.379	62.8	−0.392	79.0
hbnhn-2	−0.376	66.3	−0.394	79.9
hb2nhfC1	−0.382	68.5	−0.369	65.8
hb2nhfC2	−0.371	65.1	−0.371	65.1
pnicnn	−0.384	79.3	−0.384	79.3
complex	e (P)	σ (P)	e (N)	σ (N)
pnicpn	0.675	339.7	−0.381	79.9
pnicpf-1	0.704	280.6	−0.363	62.2
pnicpfhbnhf-1	0.738	263.2	−0.373	72.8
pnicnf	0.736	265.0	−0.377	76.7
pnicpfhbnhf-2	0.742	262.5	−0.369	70.6
pnicpf-2	0.728	276.0	−0.364	69.4
complex	e (L)[b]	σ (L)[b]	e (R)[b]	σ (R)[b]
pnicpp-fppf	0.673	354.0	0.673	354.0
pnicpp-fpph	0.649	342.8	0.767	271.4
pnicpf-tg	0.719	282.0	0.730	264.7
pnicpf-tc	0.718	279.6	0.731	259.8
pnicpf-cc	0.743	278.5	0.739	264.7
pdipC2	0.738	269.1	0.738	269.1
pdipCi	0.737	269.1	0.737	269.1
pnicpp-hpph	0.731	278.7	0.731	278.7

[a]The charges on P and N in isolated PH_2F and NH_2F are 0.735 and −0.367 e, respectively. The absolute chemical shielding on P and N in the monomers are 272.8 and 77.6 ppm, respectively. [b](L) and (R) refer to the molecules on the left- and right-hand sides of the panels in Figures 2−4.

As noted above, for complexes in which the two NH_2F molecules are inequivalent, charge transfer occurs from the molecule on the right to that on the left in Figure 2. Thus, it is important to note that although the molecule on the right loses electron density, the N atom on the right may be more negatively charged than the N on the left. The electron densities in these complexes are polarized to the left. Electron density loss comes primarily from the H atoms on the right, and the F atom on the left always gains some of this density. As a result, the charges on N and the N chemical shieldings are not well correlated. If the charge on the N atom on the right is −0.384e or greater, the chemical shielding increases relative to isolated NH_2F. This occurs in the complexes hbnhn-1, hbnhn-2, and pnicnn. However, if the charge on this N is less than

dx.doi.org/10.1021/jp3100816 | J. Phys. Chem. A 2013, 117, 183−191

Table 4. Spin−Spin Coupling Constants (Hz) Across Intermolecular Bonds in Complexes $(NH_2F)_2$, $H_2FP{:}NFH_2$, and $(PN_2F)_2$[a]

$(NH_2F)_2$	^1J(N−H)[b]	^{2h}J(N−N)	^{1h}J(H−N)	^{1p}J(N−N)	^{2h}J(N−F)	^{1h}J(H−F)
hbnhn-1	**−57.2**	**1.7**	**2.1**			
hbnhn-2	**−56.5**	**1.0**	**1.7**			
hb2nhfC1	**−56.2**				**0.5**	**−7.4**
	−56.9				**−3.5**	**−6.8**
hb2nhfC2	**−56.4**				**−0.6**	**−8.6**
pnicnn				**9.8**		
$H_2FN{:}PFH_2$	^1J(N−H)[b]	^{2h}J(N−F)	^{1h}J(H−F)	^{1p}J(P−N)	^{1p}J(P−F)	^{1p}J(N−F)
pnicpn				**−114.3**	*101.5*	*−40.3*[c]
pnicpf-1					**211.6**	
pnicpfhbnhf-1	**−56.6**	**−2.3**	**−6.6**		**43.0**	
pnicnf				*−9.5*		**−14.4**
pnicpfhbnhf-2	**−56.4**	**−0.7**	**−7.2**		**39.9**	
pnicpf-2					**237.2**	
$(PH_2F)_2$					^{1p}J(P−P)	^{1p}J(P−F)
pnicpp-fppf					**998.1**	*655.4*[d]
pnicpp-fpph					**472.5**	*232.4*[e]
pnicpf-tg					*42.3*	**200.2**
pnicpf-tc					*4.2*	**226.4**
pnicpf-cc					*−1.3*	**196.5**
pdipC2						*43.2*
pdipCi						*45.3*
pnicpp-hpph					**75.9**	

[a]Values for primary intermolecular interactions are in bold; other values are given in italics for comparison purposes. The column headings may not always correctly describe the number of bonds between the coupled atoms, but the nature of the coupled atoms is correct. The number of bonds is correctly identified in footnotes *c*, *d*, and *e*. [b]NH_2F has ^1J(N−H) = −54.5 Hz. [c]^{2p}J(N−F) at an N−F distance of 4.154 Å. [d]^{2p}J(P−F) at a P−F distance of 4.060 Å. [e]^{2p}J(P−F) involves the F atom, which forms the linear F−P···P arrangement at a P−F distance of 4.590 Å.

−0.384e, the chemical shielding decreases, even though the charge on N may be greater than it is in the monomer. The chemical shieldings of the N atoms on the left are less than that of the monomer in all of the hydrogen-bonded complexes. Only in the complex pnicnn with its N···N pnicogen bond is the chemical shielding greater than it is in the monomer, with the charge on N equal to −0.384e.

The $H_2FP{:}NFH_2$ complex pnicpn with its P···N pnicogen bond has the greatest negative charge on N, and only in this complex is the chemical shielding of N greater than it is in the monomer. In the same complex, the positive charge on P is significantly reduced, that is, the electron density at P increases significantly, and the chemical shielding increases dramatically from 273 ppm in the monomer to 340 ppm in the complex. The two complexes with P···F pnicogen bonds, pnicpf-1 and pnicpf-2, also have increased electron densities on P and chemical shieldings of 281 and 276 ppm, respectively. The remaining three complexes, pnicpfhbnhf-1, pnicpfhbnhf-2, and pnicnf, either have P···F pnicogen bonds and N−H···F hydrogen bonds, or an N···F pnicogen bond. For these, the positive charge on P is slightly greater than in the monomer, and the chemical shielding is reduced relative to the monomer.

There are three $(PH_2F)_2$ complexes with P···P pnicogen bonds, pnicpp-fppf, pnicpp-fpph, and pnicpp-hpph. The significant structural and energetic differences among these complexes are also reflected in their electron densities and chemical shieldings. pnicpp-fppf with F−P···P−F linear has higher electron densities (lower positive charges) on the P atoms and the largest chemical shieldings of 354 ppm. pnicpp-hpph has positive charges on P that are slightly less than found for the monomer, and the chemical shieldings are only slightly greater at 279 ppm. In contrast, complex pnicpp-fpph has two inequivalent molecules, one the base with P···P−H linear and the other the acid with P···P−F linear. The P atom in the base has a positive charge greater than the monomer, and a chemical shielding similar to the monomer; the P atom of the acid has the smallest positive charge among all complexes, and a chemical shielding of 343 ppm, slightly less than that of pnicpp-fppf.

The complexes with P···F pnicogen bonds, pnicpf-tg, pnicpf-tc, and pnicpf-cc, have P chemical shieldings in the base which are less than that of the monomer, ranging from 260 to 265 ppm. The P chemical shieldings in the acid are greater than the monomer, ranging from 279 to 282 ppm. The final two complexes, pdipC2 and pdipCi, have chemical shieldings of 269 ppm. Thus, it is apparent that the P and N chemical shieldings in complexes $(NH_2F)_2$, $H_2FP{:}NFH_2$, and $(PH_2F)_2$ are not simply related to the charges on these atoms but must also reflect charge distributions and overall bonding patterns in these complexes.

Spin−Spin Coupling Constants. Spin−spin coupling constants across intermolecular bonds in complexes $(NH_2F)_2$, $H_2FP{:}NFH_2$, and $(PH_2F)_2$ are reported in Table 4. Those associated with primary interactions stabilizing the complex are given in bold; other coupling constants that are of interest are given in italics. PSO, DSO, FC, and SD components of coupling constants are reported in Table S3 of the Supporting Information. From this table it is apparent that the FC terms dominate all coupling constants and are excellent approximations to corresponding ^1J(N−H), ^{2h}J(N−N), ^{1h}J(H−N), ^{1p}J(N−N), ^{1p}J(P−N), and ^{1p}J(P−P) values. Although couplings

dx.doi.org/10.1021/jp3100816 | J. Phys. Chem. A 2013, 117, 183−191

involving F are dominated by the FC terms, contributions from PSO and SD terms may or may not be negligible.

$(NH_2F)_2$. ^1J(N−H). It was noted above that with only one exception, complexes $(NH_2F)_2$ are stabilized by hydrogen bonds. ^1J(N−H) for the NFH_2 monomer is −54.5 Hz at an N−H distance of 1.018 Å. Upon formation of an N−H···N or N−H···F hydrogen bond, the N−H bond length increases slightly as ^1J(N−H) increases in absolute value to −56 or −57 Hz. Increasing ^1J(X−H) with increasing X−H distance is not an unusual pattern, particularly for complexes with relatively weak hydrogen bonds.

^{2h}J(N−N) and ^{2h}J(N−F). All two-bond coupling constants are small, with ^{2h}J(N−N) less than 2 Hz and ^{2h}J(N−F) ranging from 0.5 to −3.5 Hz. In general, two-bond coupling constants across essentially linear hydrogen bonds vary quadratically with the intermolecular distance, but even for linear bonds, ^{2h}J(N−N) coupling constants in neutral complexes are relatively small.[55] The nonlinearity of the hydrogen bonds in $(NH_2F)_2$ complexes reduces ^{2h}J(N−N) values even further and negates a correlation with the N−N distance. To further illustrate this, ^{2h}J(N−N) values have been computed for CNH:NCH at H−N−N angles of 0° and 30°, keeping all other geometric parameters fixed at their equilibrium values. ^{2h}J(N−N) decreases from only 6 Hz when the hydrogen bond is linear, to 4 Hz when the nonlinearity is 30°.

^{1h}J(H−N) and ^{1h}J(H−F). The one-bond coupling constants ^{1h}J(H−N) for complexes with N−H···N hydrogen bonds are about +2 Hz. Since the magnetogyric ratio of ^{15}N is negative and that of ^1H is positive, the reduced one-bond coupling constants ^{1h}K(H−N) are negative. For complexes with N−H···F hydrogen bonds, the one-bond coupling constants ^{1h}J(H−F) vary between −7 and −9 Hz. Since the magnetogyric ratio of ^{19}F is positive, the reduced coupling constants ^{1h}K(H−F) are negative. Negative values of reduced one-bond coupling constants indicate that these complexes are stabilized by traditional hydrogen bonds.

^{1p}J(N−N). The complex pnicnn is the least stable complex in this set, even though the N−N distance of 2.681 Å is shorter than N−N hydrogen bond distances in the other complexes. The N−N coupling constant has its largest value of 9.8 Hz for ^{1p}J(N−N) coupling across the pnicogen bond.

H_2FP:NFH_2. Coupling Across Hydrogen Bonds. H_2FP:NFH_2 complexes prefer P···N or P···F pnicogen bonds to hydrogen bonds. Only two complexes are partially stabilized by N−H···F hydrogen bonds, and these are pnicpfhbnhf-1 and pnicpfhbnhf-2. For these, ^1J(N−H) values are −56.6 and −56.4 Hz, ^{2h}J(N−F) are −2.3 and −0.7 Hz, and ^{1h}J(H−F) are −6.6 and −7.2 Hz, respectively. These values are similar to those reported for N−H···F hydrogen bonds in complexes $(NH_2F)_2$.

Coupling Across Pnicogen Bonds. The most stable H_2FP:NFH_2 complex is pnicpn, which has a P···N pnicogen bond. ^{1p}J(P−N) is −114.3 Hz at a P−N distance of 2.524 Å. P−N coupling constants have been computed for all complexes in this set, but they are significantly smaller than ^{1p}J(P−N) for pnicpn, with absolute values less than 10 Hz. On the basis of this difference, any other P−N interactions in these complexes are not considered pnicogen bonds.

The complex pnicpf-1 is stabilized by a P···F pnicogen bond and by an electrostatic interaction between P and an H atom bonded to N. pnicpf-2 is stabilized by a P···F pnicogen bond. ^{1p}J(P−F) values are 211.6 and 237.2 Hz at P−F distances of 2.780 and 2.841 Å, respectively. ^{1p}J(P−F) for complexes pnicpfhbnhf-1 and pnicpfhbnhf-2 have values of 43.0 and 39.9 Hz at P−F distances of 3.179 and 3.184 Å, respectfully. The reduced values of these coupling constants reflect the longer P−F distances in these complexes.

One complex, pnicnf, is stabilized by an N···F pnicogen bond. ^{1p}J(N−F) is −14.4 Hz at an N−F distance of 2.720 Å. There is another N−F coupling constant that should be noted, and that is ^{2p}J(N−F) for pnicpn. This coupling constant has a value of −40.3 Hz at an N−F distance of 4.154 Å, which is significantly greater than ^{1p}J(N−F) for pnicnf. This again suggests that coupling through P in an N···P−F linear arrangement is very efficient.

$(PH_2F)_2$. As noted above, six of eight complexes $(PH_2F)_2$ are stabilized by pnicogen bonds, and two are stabilized by an antiparallel alignment of molecular dipole moment vectors. The two most stable complexes, pnicpp-fppf and pnicpp-fpph, have ^{1p}J(P−P) values of 998.1 and 472.5 Hz at P−P distances of 2.471 and 2.962 Å, respectively. The least stable complex is pnicpp-hpph for which ^{1p}J(P−P) is 75.9 Hz at a P−N distance of 3.546 Å. These results are consistent with our previous studies,[22,23,27] which demonstrated that complexes with linear F−P···P−F arrangements have greater values of ^{1p}J(P−P) than complexes with linear H−P···P−H arrangements.

Three $(PH_2F)_2$ complexes are stabilized by pnicogen P···F bonds, pnicpf-tg, pnicpf-tc, and pnicpf-cc. It is interesting to note that the P−P distances in these three complexes are similar at 2.883, 2.882, and 2.886 Å, respectively, yet ^{1p}J(P−F) values vary considerably, at 200, 226, and 197 Hz, respectively. At least three factors other than the P−F distance influence the values of these coupling constants by changing the relative orientation of the lone pairs of electrons on the coupled P and F atoms. One factor is the cis or trans arrangement with respect to the intermolecular P···F bond, of the intramolecular P−F bond of the base, and the PH_2 group of the acid. The second is rotation around the intramolecular P−F bond of the base. It is well-known that such rotations influence both the signs and magnitudes of coupling constants.[56,57] The third factor is the tilt of the molecule involving the F atom which forms the P···F pnicogen bond, as measured by the P···F−P angle. This angle has values of 104, 117, and 126° for pnicpf-tg, pnicpf-tc, and pnicpf-cc, respectively. To examine the dependence of ^{1p}J(P−F) on the tilt angle, calculations have been performed on the pnicpf-tc isomer with this angle fixed at 104, 117, and 126°, keeping all other structural parameters at their equilibrium values in pnicpf-tc. ^{1p}J(P−F) values for these structures are 205, 226, and 241 Hz, respectively.

The two remaining complexes, pdipC2 and pdicCi, are stabilized primarily by an antiparallel alignment of molecular dipole moment vectors. That there are no strong pnicogen bonds is reflected by the intermolecular P−F coupling constants, which are 43.2 and 45.3 Hz at P−F distances of 3.172 and 3.176 Å, respectively. The values of these coupling constants are similar to ^{1p}J(P−F) for complexes pnicpfhbnhf-1 and pnicpfhbnhf-2, which have similar P−F distances.

■ CONCLUSIONS

Ab initio MP2/aug'-cc-pVTZ calculations have been performed to identify local minima on the $(NH_2F)_2$, H_2FN:PFH_2, and $(PH_2F)_2$ potential surfaces, to characterize the types of interactions that stabilize the complexes found at these minima, and to evaluate their binding energies. ^{15}N, ^{19}F, and ^{31}P chemical shieldings and EOM-CCSD coupling constants across intermolecular bonds have been computed for all of the

dx.doi.org/10.1021/jp3100816 | J. Phys. Chem. A 2013, 117, 183−191

complexes. These calculations support the following statements.

(1) Five equilibrium structures have been found on the $(NH_2F)_2$ surface. Four of these are stabilized by N−H···N or N−H···F hydrogen bonds. The complex with the smallest binding energy has an N···N pnicogen bond.

(2) There are eight equilibrium structures on the $(PH_2F)_2$ surface. These complexes are stabilized preferentially by P···P or P···F pnicogen bonds. Complexes with P···P bonds and at least one F−P···P arrangement linear are more stable than complexes with P···F bonds, although the complex with a P···P bond and H−P···P−H linear is the least stable complex on the surface. Two complexes stabilized by an antiparallel alignment of the dipole moment vectors of the two monomers are more stable than the complex with a pnicogen bond and H−P···P−H linear. Hydrogen-bonded complexes do not exist on this surface.

(3) Six equilibrium structures have been found on the $H_2FP{:}NFH_2$ surface. These complexes are stabilized by P···N, P···F, and N···F pnicogen bonds, with the complex with the P···N bond the most stable. Two complexes are stabilized by both P···F pnicogen bonds and distorted N−H···F hydrogen bonds.

(4) Bond critical points exist for all of the pnicogen bonds: P···P, P···F, P···N, N···F, and N···N, as well as for N−H···N and N−H···F hydrogen bonds. Bonding data indicate that the intermolecular bonds in these complexes have little covalent character. The highest degree of covalency is found for the two complexes on the $(PH_2F)_2$ surface which have P···P pnicogen bonds and at least one F−P···P arrangement that approaches linearity, and the complex on the $H_2FP{:}NFH_2$ surface that has a P···N pnicogen bond with F−P···N−F linear.

(5) Stabilizing charge-transfer transitions exist in all complexes except for the two $(PH_2F)_2$ complexes with antiparallel alignments of molecular dipole moment vectors. The largest charge-transfer energies are found for the lp P → σ^*P−F orbital for the $(PH_2F)_2$ complexes with F−P···P−F and F−P···P−H linear, and for the lp N → σ^*P−F orbital for the $H_2FP{:}NFH_2$ complex with F−P···N−F approaching linearity.

(6) For complexes in which the two molecules are inequivalent, charge transfer occurs from the base to the acid. However, the charges on N and P and the absolute N and P chemical shieldings are not well correlated. These shieldings may also reflect charge distributions and overall bonding patterns.

(7) Coupling constants ^1J(N−H) across an N−H···Y hydrogen bond increase slightly relative to NH_2F, ^{2h}J(N−Y) values are small, and ^{1h}J(H−Y) values indicate that the hydrogen bonds in these complexes are traditional hydrogen bonds. Coupling constants ^{1p}J(P−P) across P···P pnicogen bonds are large but vary significantly from 1000 Hz for the $(PH_2F)_2$ complex with F−P···P−F linear, to 75 Hz for that with H−P···P−H linear. Nevertheless, coupling constants across the same type of pnicogen bond do not correlate with corresponding intermolecular distances.

■ ASSOCIATED CONTENT

Supporting Information

MP2/aug'-cc-pVTZ structures and energies of $(NH_2F)_2$, $H_2FP{:}NFH_2$, and $(PH_2F)_2$ complexes; PSO, DSO, FC, and SD components of spin−spin coupling constants J; full refs 39, 45, and 52. This material is available free of charge via the Internet at http://pubs.acs.org.

■ AUTHOR INFORMATION

Corresponding Author

*E-mail: ibon@iqm.csic.es (I.A.); jedelbene@ysu.edu (J.E.D.B.).

Notes

The authors declare no competing financial interest.

■ ACKNOWLEDGMENTS

This work was carried out with financial support from the Ministerio de Educación y Ciencia (Project No. CTQ200913129C0202) and Comunidad Autónoma de Madrid (Project MADRISOLAR2, ref S2009/PPQ1533). Thanks are given to the Ohio Supercomputer Center for its continued support and to the CTI (CSIC).

■ REFERENCES

(1) Desiraju, G. R., Ed. *Crystal Design, Structure and Function. Perspectives in Supramolecular Chemistry*; Wiley: Chichester, U.K., 2003.

(2) Braga, D.; Grepioni, F.; Orpen, A. G., Eds. *Crystal Engineering: From Molecules and Crystals to Materials*; NATO Science Series, Ser. C; Kluwer: Dordrecht, The Netherlands, 2005; Vol. *538*.

(3) Lehn, J. M. *Chem. Soc. Rev.* **2007**, *36*, 151−160.

(4) Grabowski, S. J. *Hydrogen Bonding: New Insights*; Springer: Dordrecht, The Netherlands, 2006.

(5) Buckingham, A. D.; Del Bene, J. E.; McDowell, S. A. C. *Chem. Phys. Lett.* **2008**, *463*, 1−10.

(6) Gilli, G.; Gilli, P. *The Nature of the Hydrogen Bond. Outline of a Comprehensive Hydrogen Bond Theory*; IUCr Monographs on Crystallography, No. 23; Oxford Science Publications, Oxford University Press: Oxford, U.K., 2009.

(7) Metrangolo, P.; Resnati, G. *Halogen Bonding: Fundamental and Applications*; Structure and Bonding; Springer: New York, 2008; Vol. *126*.

(8) Grabowski, S. J. *J. Phys. Chem. A* **2012**, *116*, 1838−1845.

(9) Alkorta, I.; Sánchez-Sanz, G.; Elguero, J.; Del Bene, J. E. *J. Phys. Chem. A* **2012**, *116*, 2300−2308.

(10) Zahn, S.; Frank, R.; Hey-Hawkins, E.; Kirchner, B. *Chem.—Eur. J.* **2011**, *17*, 6034−6038.

(11) Solimannejad, M.; Gharabaghi, M.; Scheiner, S. *J. Chem. Phys.* **2011**, *134*, 024312−024316.

(12) Scheiner, S. *J. Chem. Phys.* **2011**, *134*, 094315−094319.

(13) Scheiner, S. *J. Phys. Chem. A* **2011**, *115*, 11202−11209.

(14) Adhikari, U.; Scheiner, S. *J. Phys. Chem. A* **2012**, *116*, 3487−3497.

(15) Adhikari, U.; Scheiner, S. *Chem. Phys. Lett.* **2012**, *532*, 31−35.

(16) Scheiner, S. *Chem. Phys. Lett.* **2011**, *514*, 32−35.

(17) Scheiner, S. *Chem. Phys.* **2011**, *387*, 79−84.

(18) Scheiner, S. *J. Chem. Phys.* **2011**, *134*, 164313−164319.

(19) Adhikari, U.; Scheiner, S. *J. Chem. Phys.* **2011**, *135*, 184306−184310.

(20) Scheiner, S.; Adhikari, U. *J. Phys. Chem. A* **2011**, *115*, 11101−11110.

(21) Scheiner, S. *Phys. Chem. Chem. Phys.* **2011**, *13*, 13860−13872.

(22) Del Bene, J. E.; Alkorta, I.; Sánchez-Sanz, G.; Elguero, J. *Chem. Phys. Lett.* **2011**, *512*, 184−187.

(23) Del Bene, J. E.; Alkorta, I.; Sánchez-Sanz, G.; Elguero, J. *J. Phys. Chem. A* **2011**, *115*, 13724−13731.

(24) Adhikari, U.; Scheiner, S. *Chem. Phys. Lett.* **2012**, *536*, 30−33.

(25) Li, Q.-Z.; Li, R.; Liu, X.-F.; Li, W.-Z.; Cheng, J.-B. *J. Phys. Chem. A* **2012**, *116*, 2547−2553.

(26) Li, Q.-Z.; Li, R.; Liu, X.-F.; Li, W.-Z.; Cheng, J.-B. *ChemPhysChem* **2012**, *13*, 1205−1212.

(27) Del Bene, J. E.; Alkorta, I.; Sánchez-Sanz, G.; Elguero, J. *J. Phys. Chem. A* **2012**, *116*, 3056−3060.

(28) Del Bene, J. E.; Alkorta, I.; Sánchez-Sanz, G.; Elguero, J. *Chem. Phys. Lett.* **2012**, *538*, 14−18.

(29) Alkorta, I.; Sánchez-Sanz, G.; Elguero, J.; Del Bene, J. E. *J. Chem. Theor. Comput.* **2012**, *8*, 2320−2327.
(30) Del Bene, J. E.; Alkorta, I.; Sánchez-Sanz, G.; Elguero, J. *J. Phys. Chem. A* **2012**, *116*, 9205−9213.
(31) Boese, A. D.; Chandra, A.; Martin, J. M. L.; Marx, D. *J. Chem. Phys.* **2003**, *119*, 5965−5980.
(32) Pople, J. A.; Binkley, J. S.; Seeger, R. *Int. J. Quantum Chem., Quantum Chem. Symp.* **1976**, *10*, 1−19.
(33) Krishnan, R.; Pople, J. A. *Int. J. Quantum Chem.* **1978**, *14*, 91−100.
(34) Bartlett, R. J.; Silver, D. M. *J. Chem. Phys.* **1975**, *62*, 3258−3268.
(35) Bartlett, R. J.; Purvis, G. D. *Int. J. Quantum Chem.* **1978**, *14*, 561−581.
(36) Del Bene, J. E. *J. Phys. Chem.* **1993**, *97*, 107−110.
(37) Dunning, T. H. *J. Chem. Phys.* **1989**, *90*, 1007−1023.
(38) Woon, D. E.; Dunning, T. H. *J. Chem. Phys.* **1995**, *103*, 4572−4585.
(39) Frisch, M. J.; Trucks, G. W.; Schlegel, H. B.; Scuseria, G. E.; Robb, M. A.; Cheeseman, J. R.; Scalmani, G.; Barone, V.; Mennucci, B.; Petersson, G. A.; et al. *Gaussian 09*, revision A.02; Gaussian, Inc.: Wallingford CT, 2009.
(40) Bader, R. F. W. *Atoms in Molecules: A Quantum Theory*; Pearson Education Limited: London, 1990.
(41) Popelier, P. L. A. *Atoms in Molecules: An Introduction*; Prentice Hall, Harlow, U.K., 2000.
(42) Keith, T. A. *AIMAll*, TK Gristmill Software: Overland Park, KS, 2011; see aim.tkgristmill.com.
(43) Reed, A. E.; Curtiss, L. A.; Weinhold, F. *Chem. Rev.* **1988**, *88*, 899−926.
(44) Glendening, E. D.; Badenhoop, J. K.; Reed, A. E.; Carpenter, J. E.; Bohmann, J. A.; Morales, C. M.; Weinhold, F. *NBO 5.G*; University of Wisconsin: Madison, WI, 2004.
(45) Schmidt, M. W.; Baldridge, K. K.; Boatz, J. A.; Elbert, S. T.; Gordon, M. S.; Jensen, J. H.; Koseki, S.; Matsunaga, N.; Nguyen, K. A.; Su, S. J.; et al. *Gamess*, version 11; Iowa State University: Ames, IA, 2008.
(46) Bulat, F.; Toro-Labbé, A.; Brinck, T.; Murray, J.; Politzer, P. *J. Mol. Model.* **2010**, *16*, 1679−1691.
(47) Bader, R. F. W.; Carroll, M. T.; Cheeseman, J. R.; Chang, C. *J. Am. Chem. Soc.* **1987**, *109*, 7968−7979.
(48) Ditchfield, R. *Mol. Phys.* **1974**, *27*, 789−807.
(49) Perera, S. A.; Nooijen, M.; Bartlett, R. J. *J. Chem. Phys.* **1996**, *104*, 3290−3305.
(50) Perera, S. A.; Sekino, H.; Bartlett, R. J. *J. Chem. Phys.* **1994**, *101*, 2186−2196.
(51) Schäfer, A.; Horn, H.; Ahlrichs, R. *J. Chem. Phys.* **1992**, *97*, 2571−2577.
(52) Stanton, J. F.; Gauss, J.; Watts, J. D.; Nooijen, M.; Oliphant, N.; Perera, S. A.; Szalay, P. S.; Lauderdale, W. J.; Gwaltney, S. R.; Beck, S.; et al. *ACES II*; University of Florida: Gainesville, FL.
(53) Andrews, L.; Lascola, R. *J. Am. Chem. Soc.* **1987**, *109*, 7020−7024.
(54) Dréan, P.; Paplewski, M.; Demaison, J.; Breidung, J.; Thiel, W.; Beckers, H.; Bürger, H. *Inorg. Chem.* **1996**, *35*, 7671−7678.
(55) Del Bene, J. E.; Bartlett, R. J. *J. Am. Chem. Soc.* **2000**, *122*, 10480−10481.
(56) Karplus, M. J. *Chem. Phys.* **1959**, *30*, 11−15.
(57) Del Bene, J. E.; Elguero, J. *J. Phys. Chem. Lett.* **2006**, *111*, 12543−12545.